- Technical Paper -

STUDY ON THE IN-PLANE FAILURE MECHANISMS AND STRENGTH EVALUATION OF RC FRAMES WITH CLT INFILL

Ahmad Ghazi ALJUHMANI[*1], Hamood ALWASHALI[*2], Masaki MAEDA[*3], and Matsutaro Seki[*4]

ABSTRACT

The objective of this study is to clarify the possible failure mechanisms and strength of RC frames with CLT infill and to investigate the CLT panel compression strut width. Simplified strength evaluation was summarized based on a literature review of the RC frames with different material infills. Diagonal tests of CLT panels and FE analysis of RC frames with CLT infill system were conducted in order to clarify the change of failure mechanisms based on the strut width and the relative stiffness for the RC frame and CLT. It was found that brittle failure mechanisms could be avoided by properly designing the RC-CLT system.

Keywords： RC buildings, Cross-laminated Timber, CLT infill, Seismic retrofit, FEM

1. INTRODUCTION

Hybrid RC and timber structures are getting more attention, and their numbers are increasing rapidly as an eco-friendly solution to contribute towards the sustainable societies prescribed in the UN's Sustainable Development Goals (SDGs). Cross-laminated timber (CLT) has relatively high shear strength, is lightweight, and has low carbon emission. Using CLT panels as shear walls in RC or steel structures can increase the seismic capacity of the building with also securing lower seismic demand due to CLT's low mass, resulting in improving not only the lateral strength of the structure but also its ductility. However, the insertion of CLT panels in the RC frames could also lead to unwanted failure mechanisms (e.g., brittle failure). Therefore, it is essential to understand and investigate the possible failure mechanisms and seismic behaviour of these structures.

Recently in Japan, RC frames or steel frames with CLT infill buildings were constructed, as shown in Fig. 1. Worldwide, several researchers have started investigating the effect of CLT infill on RC or steel frames. A parametric study on different types of steel frames with CLT infill using static pushover analysis was carried out by Dickof et al. [1] to clarify the ductility and overstrength values. It was found that CLT infill is effective in the case of lower ductility frames, whereas it does not have much influence in the case of ductile frames. [1] focused only on the influence of CLT infill on the ductility factor and the increase of strength for the RC frame. However, the possible failure mechanism, as well as an evaluation method, were not considered in [1]. Another numerical simulation has been carried out by Stazi et al. [2] to understand the effect of CLT infill on RC frames. This study also focused only on the overall influence of the CLT panel on the increase of the strength and stiffness of the RC frame. Several experiments on five 1/3 scale RC frames with different CLT infill types were conducted by Haba et al. [3]. In [3], even though several specimens with the same RC frame and CLT panels with different specifications were tested, only one failure was observed, which is a shear failure in the RC columns. In all the previous studies, researchers have only investigated the increase in strength and ductility of the frame due to the insertion of the CLT panel. However, research on the different possible failure mechanisms is still lacking, and evaluation guidelines and standards for engineering practice are still unavailable. Therefore, the objectives of this study are:

1. Clarify the possible in-plane failure mechanisms and strength evaluation of RC frames with CLT panels infill.
2. Investigate the expected compression strut width of the CLT panel and evaluate its seismic capacity.
3. Investigate the effect of different parameters (e.g., compression strut width and CLT-to-RC connections) on the expected failure of RC frame with CLT infill system.

Fig. 1 Examples of steel frame with CLT infill (left) [4], RC frame with CLT infill (right) [5] buildings

2. Expected failure modes and capacity evaluation

Although CLT Infill in RC frames is a new concept, infill walls or post-installed walls are a common practice, such as masonry infill walls, RC walls, or steel braces. The main difference is that the material properties of the CLT panel are different, which may completely alter the RC frame performance compared to other conventional methods, and this has not been

*1 Graduate student, Dept. of Architecture and Building Science, Tohoku University, JCI Student Member
*2 Associate Prof., Graduate School of Environmental and Life Science, Okayama University, Dr. Eng., JCI Member
*3 Professor, Dept. of Architecture and Building Science, Tohoku University, Dr. Eng., JCI Member
*4 Visiting Research Fellow, Building Research Institute, Dr. Eng., JCI Member

investigated in past studies. In this section, the possible failure mechanisms of RC frames with CLT infill systems are investigated based on previous research or based on comparisons with other infill materials.

2.1 Column shear failure

This failure was observed in Haba et al. [3] experiments (Fig. 2). 1/3 scale specimen with CLT panels along the entire width of the frame (1540 mm) was tested. The height of the CLT infill was 840 mm, and it was fixed with the RC frame using epoxy resin. Two panels of Japanese Cedar CLT (Mx60b-3-3 grade) were used with 60 mm thickness (30 mm for each panel). In this case, the RC columns are shear-critical columns (shear capacity for the RC columns is less than the flexural capacity). Thus, the frame does not have enough deformation capacity for the CLT infill to fail first, and the dominant failure will be columns shear failure.

In this case, maximum strength capacity can be estimated by adding three components: the strength of the two RC columns and the strength of connections at the top of the CLT panel. It can be calculated using Eq. 1. with reference to Fig. 3.

$$Q_{sh} = 2 \times Q_{su} + Q_{joint} \quad (1)$$

Where Q_{su} is the column shear strength calculated as prescribed in AIJ code [6] or any other adequate method or code, and Q_{joint} is the strength of the CLT to RC joint on top. If there are no connections between the CLT panel and the RC frame, then Q_{joint} can be ignored.

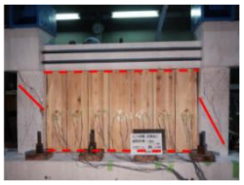

Fig. 2 Column shear failure in as observed in [3]

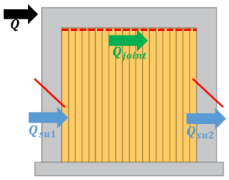

Fig. 3 Column shear failure for RC frame with CLT

2.2 Punching shear failure

Having relatively strong and very stiff walls within an RC frame could cause a punching shear failure, which is observed in RC frames with strong steel braces as in Ishimura et al. [7] (Fig. 4). It was also observed in RC frames with masonry infill that were retrofitted by ferrocement, such as in the Sen et al. experiment [8]. This failure could happen in the case of a very strong CLT infill relative to the surrounding RC frame. In this case, maximum strength capacity can be estimated by adding three components. The first component is the RC column (windward) which has punching shear failure. The second component is connections at the top of CLT panel and RC beam. The third component is the leeward RC column, which could fail in either shear or flexural, and can be calculated by Eq. 2. with reference to Fig. 5.

$$Q_{pun} = PQ_{c1} + Q_{joint} + min(Q_{su}, Q_{mu}) \quad (2)$$

Where PQ_{c1} is the punching shear capacity of the first column as prescribed in JBDPA [9], Q_{su} is column shear strength, and Q_{mu} is column flexural strength.

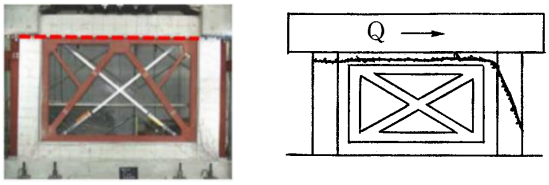

Fig. 4 Punching shear failure in as observed in [7] (left); and as mentioned in JBDPA [9] (right)

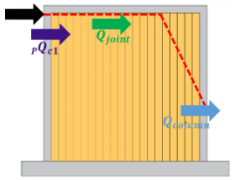

Fig. 5 Punching shear failure for RC with CLT

2.3 Frame overall flexural failure

This failure could occur when the CLT infill is stiff relative to the RC frame, and the CLT panel is strongly connected with the RC frame. In this case, the RC frame and CLT panel will act as a single component similar to a cantilever flexural wall. There are no experimental tests of RC frames with CLT infill having overall flexural failure. However, similar behaviour is observed with other infilled walls, such as tests by Lucas et al. [10] on RC frames with post-installed RC walls (Fig. 6), as well as masonry infills such as Sen et al. [8]. In this failure, maximum strength capacity can be estimated by the overall flexural capacity (Q_{fl}) as a cantilever flexural wall as shown in Fig.7. The maximum strength could be calculated using Eq. 3 and Eq. 4 that are adopted from JBDPA [9] with reference to Fig.7.

$$Q_{fl} = M_u / h_0 \quad (3)$$

$$M_u = a_t f_y l_c + 0.5 N l_c \quad (4)$$

Where M_u is moment capacity, h_0 is the clear height of the column, a_t is longitudinal reinforcement area for one column, f_y is the yield strength of column's longitudinal reinforcement, l_c is the distance between the centers of the boundary columns, and N is the total axial load applied on the entire frame. It should be noted here that the maximum strength is calculated entirely based on the RC frame strength. There is no contribution for the CLT panel by assuming there are no tension connections between the CLT panel and the RC frame at the bottom. If connections are added at the bottom of the CLT panel, then the tensile of the CLT panel could also contribute to the flexural capacity and need to be added to Eq. 4.

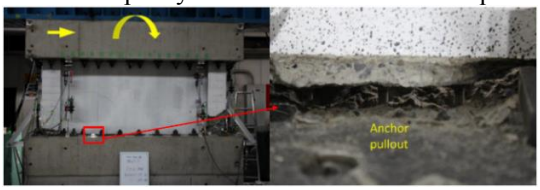

Fig. 6 Overall flexural failure as observed in [10]

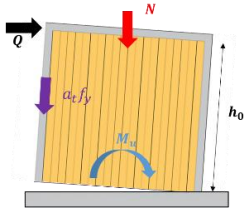

Fig. 7 Overall flexural failure for RC frame with CLT

2.4 CLT panel shear failure

No experimental studies are showing shear failure of CLT walls in RC frames. However, other infill materials such as masonry infill walls in RC frames had a shear failure, such as those shown in Fig. 8. For CLT infill, it could occur in a ductile RC frame with relatively lower stiffness for CLT. In this case, the columns are flexural columns (flexural capacity is less than the shear capacity). Thus, the frame has enough deformation capacity for the CLT infill to deform, and the dominant failure will be CLT failure. Capacity can be calculated by adding the flexural strength of the two columns to the shear strength to the CLT panel itself, as shown in Eq. 6 and Eq. 7 with reference to Fig.9. It should be noted here that Q_{mu} needs to be calculated assuming the clear height h_0 to be around half of the column clear height.

$$Q_{CLT-s} = Q_{mu1} + Q_{mu2} + S_{CLT} \quad (6)$$

$$S_{CLT} = \tau_{CLT} \times L_{CLT} \times t_{CLT} \quad (7)$$

Where Q_{mu1} and Q_{mu2} are windward and leeward column capacity, S_{CLT} is CLT panel shear capacity, and τ_{CLT}, L_{CLT}, and t_{CLT} are CLT panel shear strength, length, and thickness, respectively.

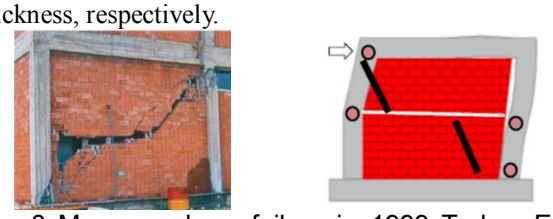

Fig. 8 Masonry shear failure in 1999 Turkey EQ (left) [11], and as observed in Sen et al. [8] (right)

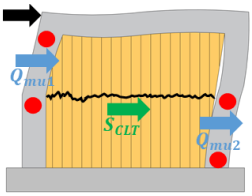

Fig. 9 CLT shear failure for RC with CLT infill

2.5 CLT panel compression failure

There are no experimental studies showing the failure of CLT diagonal compression failure in RC frame. However, other infill materials in RC frames, such as masonry walls, had a shear failure, such as those shown in Fig. 10. This failure was observed in the experiment done by Alwashali et al. [12] on masonry infill, and it is thought that CLT infill could also have a similar failure mechanism. This failure is similar to the CLT panel shear failure; however, in this case, CLT compression capacity (C_{CLT}) is less than CLT shear capacity (S_{CLT}).

This failure capacity can be calculated by Eq. 8 and Eq. 9 with reference to Fig. 11.

$$Q_{CLT-c} = Q_{mu1} + Q_{mu2} + C_{CLT} \quad (8)$$

$$C_{CLT} = \sigma_{CLT} \times W_{strut} \times t_{CLT} \times \cos\theta \quad (9)$$

Where C_{CLT} is CLT panel shear capacity, σ_{CLT} is CLT panel compressive strength, W_s is compression strut width with, θ is the angle between RC base and the strut with reference to Fig. 11. The estimation of the strut width (W_s) is a complex topic that has not been studied previously for CLT infills. The following section will investigate the strut width based on simple diagonal compression tests and finite element analysis.

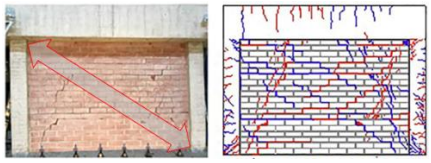

Fig. 10 Compression strut failure as found in [12]

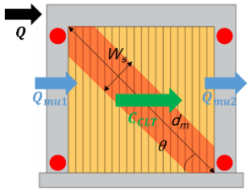

Fig. 11 CLT shear failure of RC frame with CLT infill

3. Compression strut width of CLT panel

3.1 Compression strut mechanism

The capacity evaluation for all the failure mechanisms mentioned above, except CLT compression strut failure, is relatively well understood and thought that could be directly applied. However, in the case of CLT compression strut failure, strut width is the value that depends on materials characteristics, thus might differ from other infill materials. In the case of CLT infill, no calculation approaches nor empirical equations were proposed for strut width. One simple approach is to assume the methods used for masonry infill might also be applicable for CLT infill. In this study, the two methods by FEMA-306 [13] and Sen et al. [8] only are compared. The values of strut width to the diagonal length that are calculated by the two methods for different flexural relative stiffness (frame flexural stiffness divided by CLT panel flexural stiffness) are shown in Fig. 12. The calculations of strut width by [8] and [13] showed large variations, as can be seen in Fig. 12. This could lead to uncertainty in estimating strength by the failure mechanism of the compression strut.

In order to adequately estimate the strut width of CLT infill in the RC frame, simple diagonal tests were conducted, and then finite element models were developed and validated by the diagonal test. The FE analysis is then used to simulate the CLT infill in the RC frame to estimate the compression strut width.

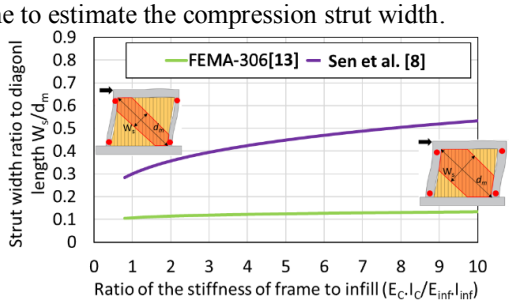

Fig. 12 Strut width relation with relative flexural stiffness of RC frame to CLT infill

3.2 Diagonal compression test

The interaction between the CLT infill panel and the RC frame under lateral forces is shown in Fig. 13. The transmitted forces to the CLT panel at the corner of the actual RC frame could be reproduced using diagonal compression test configuration, as shown in Fig. 14. Therefore, this test-set up was used to obtain the characteristics of CLT panels under compression forces.

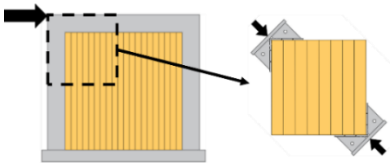

Fig. 13 Behaviour of CLT panel under lateral load

3.2.1 Experimental test

Hydraulic Jack was used to apply a monotonic vertical downwards force on 1200 mm by 1200 mm CLT panel (loading rate in the range of 0.15~0.2 mm/s). Three replicates were tested, and all the panels were 5-layer 150 mm thick panels made from Japanese cedar with Mx-60-5-5 grade. Each panel was installed vertically between two steel 'shoe' caps (Fig. 14), which were designed to distribute the load such that local bearing failure of the CLT panel does not occur. LVDTs were attached along the two diagonals of the CLT panel to calculate shear deformation. Shear deformation was calculated using Eq. 10 with reference to Fig. 15.

$$\gamma = \frac{\Delta x + \Delta y}{900 \times \sqrt{2}} \qquad (10)$$
$$\delta = \gamma \times 1200$$

Where Δx and Δy are the values obtained from the horizontal and the vertical overall LVDTs, respectively.

In addition, digital image correlation (DIC) was also used in the tests, as shown in Fig. 16, and analyzed using the DIC Software Opteca [14].

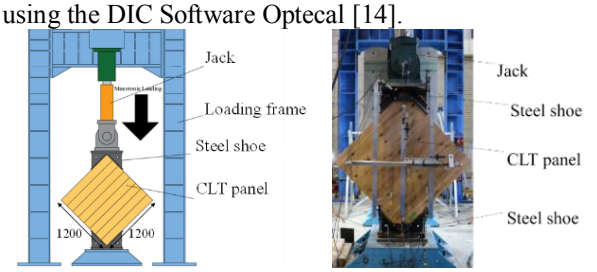

Fig. 14 Loading set-up of the compression test

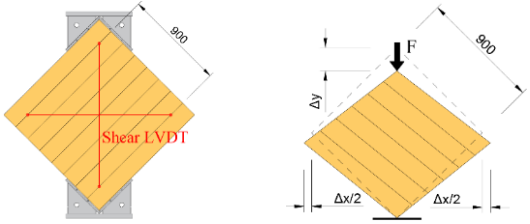

Fig. 15 LVDTs set-up and shear deformation

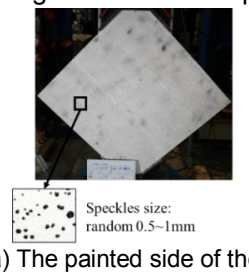

a) The painted side of the specimen for DIC

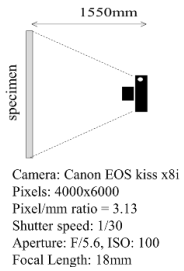

b) Location of the camera

Fig. 16 The details of the DIC set-up

3.2.2 FEM model for diagonal compression test

A numerical model was created using the FEM software Abaqus [15]. The CLT panel was modelled as a solid element. The model consists of five layers, and the interaction between each CLT layer was assumed to be a tie constrain with no slip. Each layer was modelled as an elastic orthotropic material with three directions (L, R, T): longitudinal (in the direction of the grain), radial, and tangential. Each CLT layer has an axis orientation perpendicular to the adjacent layers. The mechanical properties of each layer are shown in Table 1, which was adopted from Japanese Wood Industry Handbook [16].

Table 1 Japanese Cedar material properties [16]

Species	Young modulus (MPa)			Shear modulus (MPa)			Poisson ratio		
	E_L	E_R	E_T	G_{LT}	G_{LR}	G_{RT}	ν_{LT}	ν_{LR}	ν_{RT}
Japanese cedar	8700	620	260	460	650	15	0.58	0.405	0.901

3.2.3 Validate FEM results with experiment results

A comparison between shear displacement-shear force curves for FE model and experiment is shown in Fig. 17. The stiffness obtained from the FE model (100.4 kN/mm) was relatively close values to the average value from experiment (106.3 kN/mm). A comparison between the strain obtained from the experiment by DIC and FEM results is shown in Fig. 18. In this case, horizontal (ε_x) and vertical (ε_y) axial strain distribution were compared at the point just before maximum load P_{max}. Overall, the strain distribution is similar in both FEM and DIC, showing that the response is governed by one main compressive strut, indicating that FEM can capture the general stress paths and give close strain values.

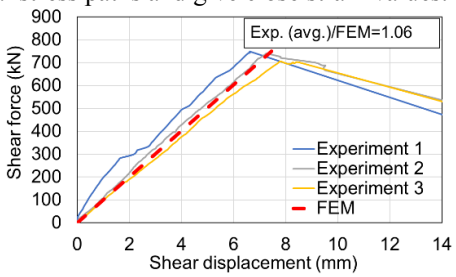

Fig. 17 Comparison between FEM and experiments

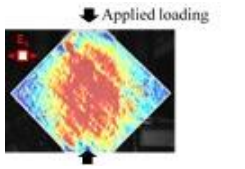

a) strain ε_x DIC experiment

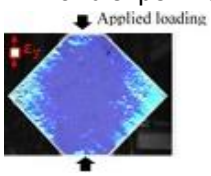

b) strain ε_y DIC experiment

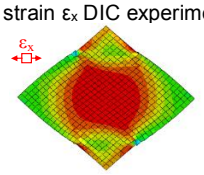

c) strain ε_x for FEM

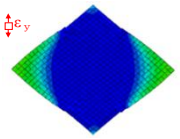

d) strain ε_y for FEM

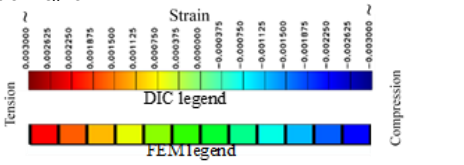

e) strain legend used in DIC and FEM for both ε_x and ε_y

Fig. 18 Comparison between FEM and DIC

3.3 FEM model for RC frame with CLT infill

3.3.1 model description

FEM software Abaqus [15] was used to model the RC frame with CLT infill. Only concrete was modeled with elastic solid elements for simplicity since the main focus is the strut width in the CLT infill. Young's

modulus and Poisson's ratio for RC were taken as 23000 MPa and 0.2, respectively. The CLT model was similar to the model used in the diagonal compression model (section 3.2.2). The frame was fixed in all directions at the bottom and free at the top. The interaction between the CLT panel and the RC frame was assumed as hard contact with no penetration between the CLT and RC elements with no friction interaction. A total of 10 frames was modelled, and the difference between each model is the relative flexural stiffness between the RC columns and the CLT infill (infill thickness was fixed, and the RC columns dimensions were increased).

3.3.2 Results and compression strut calculation

Regarding stiffness increase due to the CLT infill, the initial stiffness of bare frame F1 (the frame with the smallest relative stiffness) was 17.5 kN/mm, and stiffness increased to 75.4 kN/mm after adding the CLT infill with an increase of about 4.3 times. The initial stiffness of bare frame F15 (the frame with the largest relative stiffness) was 121.9 kN/mm, and stiffness increased to 185.9 kN/mm after adding the CLT infill with an increase of about 1.5 times. The results of strain in the diagonal strut direction for the F1 frame and F15 frame are shown in Fig. 19. Although the strain values differ slightly between these two frames, the strut width almost does not vary much. In order to compare quantitative values of the strut width, a method proposed by Jin et al. [17] was used. In this FEM analysis, a total of 12 sections were taken, and, for each section, the average strain was calculated by taking the equivalent strain area for the actual strain curve as shown in Fig. 20.

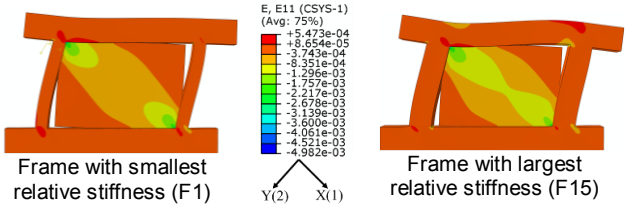

Fig. 19 Normal strain in X-direction (strut direction)

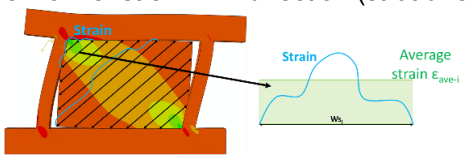

Fig. 20 Strut sections and average strain calculations

The strut width obtained from the FEM analysis for different relative RC to CLT stiffness is shown in Fig. 21. In Fig. 21, The strut width ranges between $0.34d_m$ and $0.36d_m$ with different relative RC to CLT stiffness. When also compared to the two masonry infill methods [8,13], it was found that FEM analysis has a similar tendency with FEMA-306 [13] for masonry infill; however, FEM analysis gave larger strut width values.

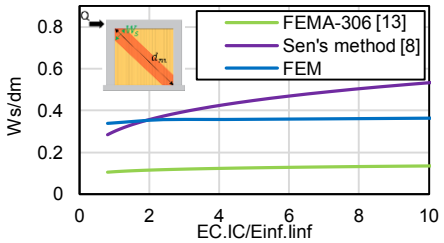

Fig. 21 Strut width: FEM vs. Masonry methods

4. Capacity evaluation of specific RC frame

In this study, the lateral strength of RC frame with CLT infilled (Q_{cal}) is proposed to be calculated by taking the minimum of the calculated lateral capacity based on the five different failure mechanisms discussed previously in section 2, as shown in Eq. 11.

$$Q_{cal} = min(Q_{sh}, Q_{pun}, Q_{fl}, Q_{CLT-c}, Q_{CLT-s}) \quad (11)$$

A case study of RC frame tested in Alwashali et al. [12] with masonry infill (specimen F-1.5) will be presented to understand the failure mechanisms well. This RC frame will be used here, assuming CLT infill as shown in Fig. 22. The thickness of the CLT panel is assumed to be 60 mm, and shear and compression strength for CLT are assumed to be 4.1 MPa and 174 MPa, respectively. These values are based on the material tests conducted before the diagonal compression test presented in section 3.2.1.

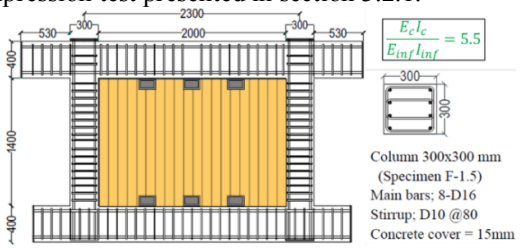

Fig. 22 Case study on RC frame for capacity evaluation (from Alwashali et al. [12])

A comparison between several methods for only the compression failure strength of the case study frame is shown in Fig. 23. It should be noted that deformation capacity evaluation is out of the scope of this paper, and thus the story drift axis in Fig. 23 and Fig. 24 is used for illustration only. As shown in Fig. 23, there is a large variation between the estimation of maximum strength for the diagonal compression failure considering previous studies for different materials such as masonry infill. This uncertainty and the lack of CLT strut width experiments will lead to significant variations in the expected strength capacity and failure mechanisms.

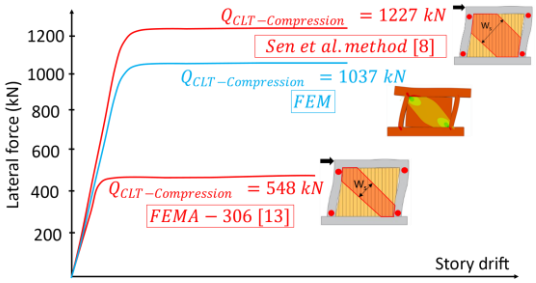

Fig. 23 Failure strength for the case study frame

The expected lateral strength capacity of the case study frame for all the five expected failure mechanisms is as shown in Fig. 24. Three shear connections were assumed at the top and at the bottom of the CLT infill to make the example shown here more practical. This number was also assumed to avoid punching shear failure. Each shear connection has a shear strength of 80 kN (total of 240 kN as Q_{joint} in Eq. 2). For CLT compression strut failure, the FEMA 306 [13] (for masonry) and FE analysis results (presented in this study) were used to calculate the strut width. As shown

in Fig. 24, compression failure gives the minimum strength value and is expected in a case assuming the strut width of masonry as in FEMA-306 [13]. However, in the case of strut width obtained from the FE analysis, the capacity of compression failure increased, and thus punching shear failure becomes the most probable failure type. The influence of the strut width is crucial in the seismic design since it affects not only the maximum capacity but also the expected seismic behaviour, which could change the behaviour from desirable ductile failure to undesirable brittle punching shear failure. Experimental verification and investigation to understand the behaviour of CLT infills are still needed.

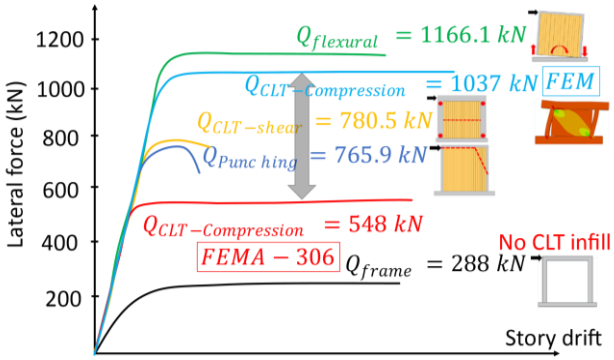

Fig. 24 Calculated capacity of the case study frame

5. CONCLUSIONS

This study presented different expected failure modes for RC frames with CLT infill based on previous studies and observations for RC frames with other infills. Also, a FEM model was developed and verified by component compression test to study the effect of CLT compression strut width on the expected failure. The main conclusions are as follows:

1. Five different possible failure modes for RC frames with CLT infill were summarized based on a literature review for RC frames with other material infills.
2. Seismic capacity and in-plane failure mechanism of RC frames with CLT infill could be predicted based on the evaluation method presented in this paper.
3. Compression strut width methods for RC frames with masonry infill have big variations when used with CLT.
4. FEM analysis showed that the compression strut width does not change much by changing the relative stiffness of the RC frame and the CLT infill (the margin was between 0.34 and 0.36 of the strut length).
5. CLT compression strut width and CLT-to-RC shear connections could significantly affect the probable failure mechanisms, changing it from ductile to brittle failure. Therefore, further experimental investigations are needed to predict the probable failure mechanism.

ACKNOWLEDGEMENT

The study was partly supported by JSPS KAKENHI Grant Number 21K14283 (Principal investigator: Hamood Alwashali, Tohoku University).

REFERENCES

[1] Dickof, C., Stiemer, S.F., Bezabeh, M.A. and Tesfamariam, S., 2014. CLT–steel hybrid system: Ductility and overstrength values based on static pushover analysis. Journal of Performance of Constructed Facilities, 28(6), p.A4014012.

[2] Stazi, F., Serpilli, M., Maracchini, G. and Pavone, A., 2019. An experimental and numerical study on CLT panels used as infill shear walls for RC buildings retrofit. Construction and building materials, 211, pp.605-616.

[3] Haba, R., Kitamori, A., Mori, T., and Fukuhara, T., 2016. Development of clt panels bond-in method for seismic retrofitting of RC frame structure. J. Struct. Constr. Eng, 81, pp.1299-1308.

[4] Xtech 2019, accessed 30 December 2021, <https://xtech.nikkei.com/atcl/nxt/mag/na/18/00076/100200003/>.

[5] Shimizu corporation, accessed 30 December 2021, <https://www.shimz.co.jp/company/about/news-release/2019/2018044.html>.

[6] AIJ, 2016. AIJ Standard for Lateral Load - Carrying Capacity Calculation of Reinforced Concrete Structures.

[7] Ishimura, M., Sadasue, K., Miyauchi, Y., and Yokoyama, T., 2012, September. Seismic performance evaluation for retrofitting steel brace of existing RC building with low-strength concrete. In Proc. of the 15th World Conf. on Earthquake Engineering, 15th WCEE (pp. 24-28).

[8] Sen, D., Alwashali, H., Tafheem, Z., Islam, M. S., and Maeda, M., 2020, September. Experimental investigation and capacity evaluation of Ferro-cement laminated masonry infilled RC frame. In Proc. of the 17th WCEE.

[9] JBDPA/The Japan Building Disaster Prevention Association, 2001. Standard for seismic evaluation of existing reinforced concrete buildings.

[10] Laughery, L., Ichinose, T., Maeda, M., Alwashali, H., Takahashi, H., Hanzawa, M., Okada, T., Ide, A. and Sonn, K., A potential vulnerability in high-strength reinforced concrete shear wall retrofits.

[11] Bachmann, H. and Suisse. Office fédéral de l'environnement, 2003. Seismic conceptual design of buildings: basic principles for engineers, architects, building owners, and authorities. SDC.

[12] Alwashali, H., and Sen, D., 2019. Experimental investigation of influences of several parameters on seismic capacity of masonry infilled reinforced concrete frame. Engineering Structures, 189.

[13] Federal Emergency Management Agency, 2013. Evaluation of earthquake damaged concrete and masonry wall buildings. FEMA.

[14] Optecal: Digital Image Correlation software 2020.

[15] Dassault Systemes Simulia Corp., Abaqus software.

[16] Basic theory of wood structure: Architectural Institute of Japan: Wood Industry Handbook.

[17] Jin, K., Choi, H. and Nakano, Y., 2016. Experimental study on lateral strength evaluation of unreinforced masonry-infilled RC frame. Earthquake Spectra, 32(3), pp.1725-1747.